Electronic Supplementary Material (ESI) for Physical Chemistry Chemical Physics.

Electronic supplementary information (ESI)

Interfacial and thermal energies driven growth and evolution of Langmuir-Schaefer monolayers of Au-nanoparticles

Mala Mukhopadhyay and S. Hazra*

Saha Institute of Nuclear Physics, 1/AF Bidhannagar, Kolkata 700064, India

$\Pi - A$ isotherm of DT-AuNP Langmuir monolayer

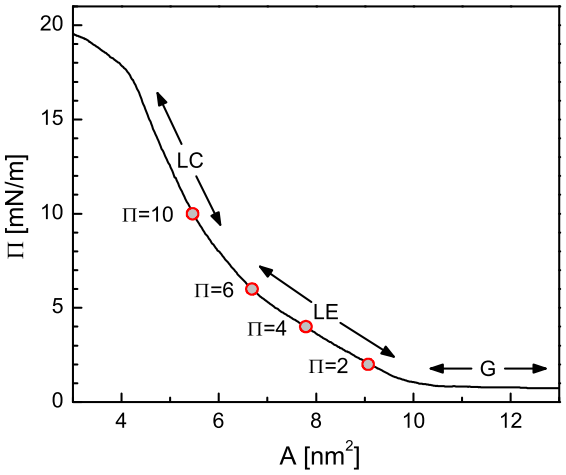

Fig. S1 Pressure-area ($\Pi - A$) isotherm of the DT-AuNP layer, recorded in a Langmuir trough, showing various phases, namely gaseous (G), liquid-expanded (LE) and liquid-condensed (LC) as reported before (in Ref. 1).

The pressure-area ($\Pi - A$) isotherm of DT-AuNP Langmuir monolayer was reported before (in Ref. 1). In short, a 1.5 ml toluene solution of DT-AuNPs (0.5 mg ml^{-1}) was spread uniformly, using a micropipette, on the surface of Milli-Q water in a Langmuir trough (KSV 5000). It was kept undisturbed for some time to let the toluene evaporate and the hydrophobic DT-AuNPs lay suspended at the air-water interface (at 23°C). Typical $\Pi - A$ isotherm of DT-AuNP Langmuir monolayer on water surface, as reported before (in Ref. 1), is shown in Fig. S1. Gaseous (G), liquid-expanded (LE) and liquid-condensed (LC) phases, corresponding to the isotherm, are indicated in Fig. S1. Also the four different pressure, where LS films were deposited, are marked in Fig. S1. It can be noted that the estimation of transfer ratio from area variation in this system, where the Langmuir monolayer is formed through network-like structure, is unreasonable. The network-like structure restricts the

fast in-plane diffusion of the DT-AuNPs towards the transferred area. Hence the barrier movement (which provides area variation) is restricted.

Bearing plots of the AFM images

The topography of the DT-AuNP/H-Si LS films obtained after evolution at ambient conditions were presented before (in Ref. 1), where 2D-network of disk-like islands of monolayer height on H-Si substrates were very much evident. The bearing plots of the AFM images, which represent the coverage of the voids and the materials (of different heights) in the films better, are shown in Fig. S2 (for two films deposited at low and high pressure), for comparison. The voids in the DT-AuNP/H-Si LS films are found more compared to the DT-AuNP/OTS-Si LS films. For $\Pi = 10$ mN m^{-1}, the voids in the DT-AuNP/OTS-Si LS film (Fig. 2) is negligible, while that in the DT-AuNP/H-Si LS film (Fig. S2) is appreciable. Also the heights of the monolayer with respect to the voids in the DT-AuNP/H-Si LS films are found less compared to the DT-AuNP/OTS-Si LS films. The difference is prominent for the DT-AuNP/H-Si LS film deposited at $\Pi = 2$ mN m^{-1}. Such observed differences in the voids and heights in the films are related to the substrate natures (attraction, instability and oxide growth), which are different for OTS-Si and H-Si substrates.

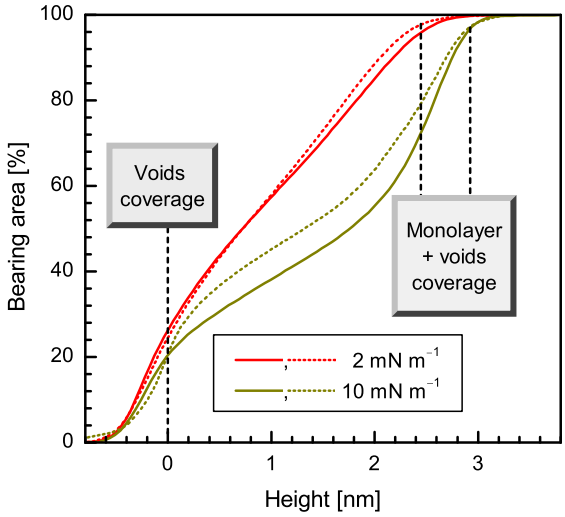

Fig. S2 Bearing plots (as obtained from AFM images in Ref. 1) of the time evolved DT-AuNP/H-Si LS films deposited at two different surface pressure (Π) showing the voids coverage and monolayer (including voids) coverage, as indicated.

Integrated EDP

The EDP of the film, $\rho_F(z)$, can be expressed as the summation of Gaussian peaks:

$$\rho_F(z) = \sum_j \rho_{0j} \exp\left[-\left(\frac{z - z_{0j}}{\sigma_0}\right)^2\right], \tag{S1}$$

where ρ_{0j} is the peak value, z_{0j} is the position and σ_0 is the standard deviation or width related term of the jth Gaussian peak. As σ_0 is fixed and same (here 1.04 nm) for all j values, the integrated EDP (Int EDP) can be expressed as

$$\text{Int EDP} = \sqrt{\pi}\sigma_0 \sum_j \rho_{0j}, \tag{S2}$$

i.e.

$$\text{Int EDP} \propto \sum_j \rho_{0j}. \tag{S3}$$

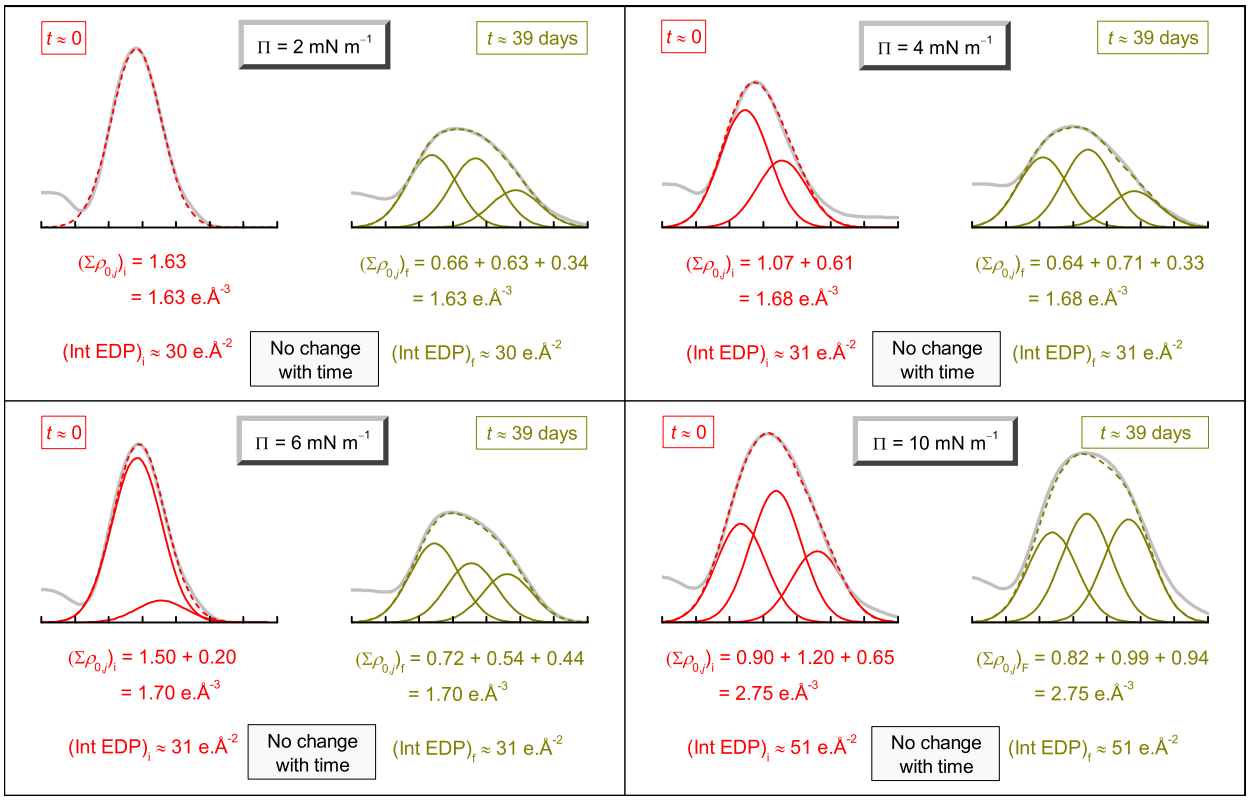

Fig. S3 Initial ($t \approx 0$) and final ($t \approx 39$ days) EDPs of the DT-AuNP/OTS-Si LS films deposited at different surface pressure (Π) and their Gaussian deconvolution. Gray profiles are the EDPs obtained from the XR data analysis, while dashed profiles are the summation of the Gaussian profiles. The summation of the Gaussian peak intensities and the corresponding integrated EDP (Int EDP) for each EDP are indicated, showing no change with time.

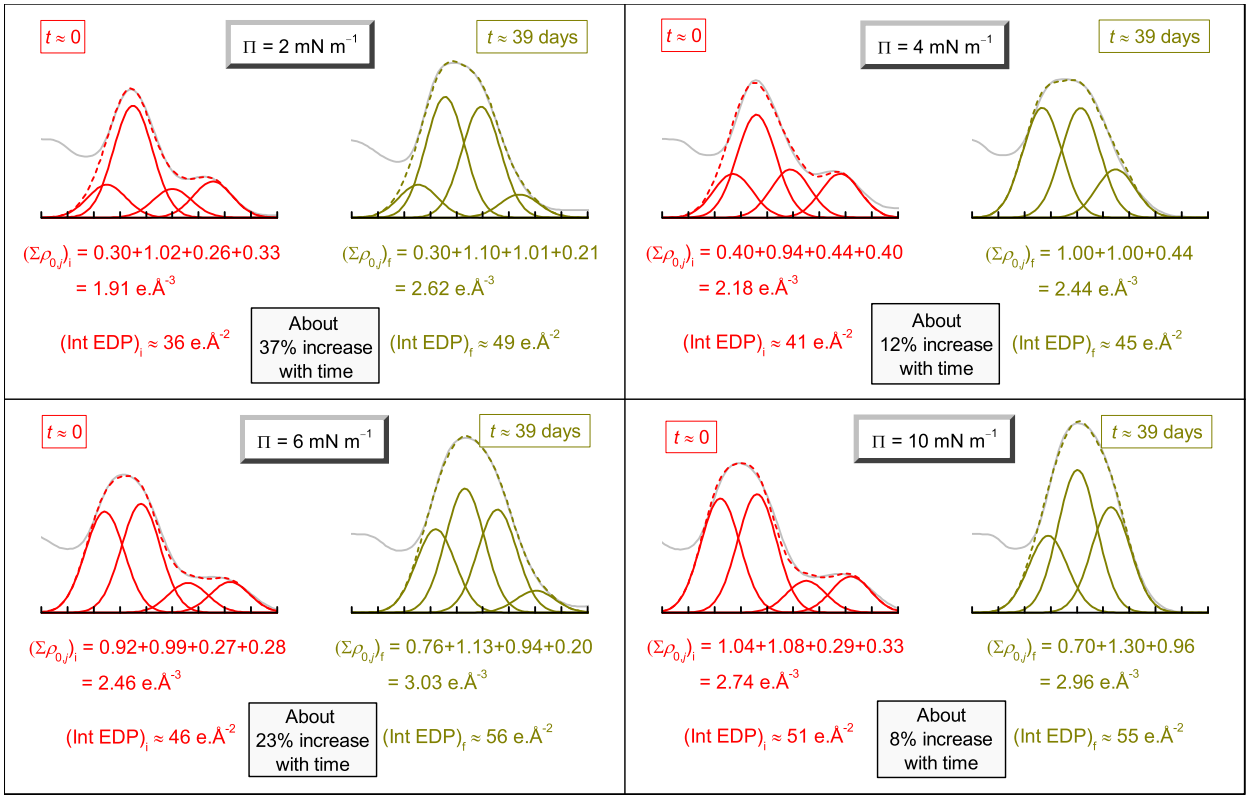

Fig. S4 Initial ($t \approx 0$) and final ($t \approx 39$ days) EDPs and their Gaussian deconvolution of the DT-AuNP/H-Si LS films deposited at different surface pressure (Π). Gray profiles are the EDPs obtained from the XR data analysis, while dashed profiles are the summation of the Gaussian profiles. The summation of the Gaussian peak intensities and the corresponding integrated EDP (Int EDP) for each EDP are indicated, showing increase with time.

EDPs of the DT-AuNP/OTS-Si and DT-AuNP/H-Si LS films of different Π values at initial ($t \approx 0$) and final ($t \approx 39$ days) stages and their Gaussian deconvolution are shown in Figs. S3 and S4. The EDP obtained using Eq. S1 (dashed profile) agrees well with the EDP obtained from X-ray data analysis (gray profile). The values of $\sum_j \rho_{0j}$ and corresponding values of Int EDP (obtained from Eq. S2) for each EDPs are indicated in Figs. S3 and S4. It is clear that with time the Int EDP remains unchanged in the DT-AuNP/OTS-Si LS films, while increases in the DT-AuNP/H-Si LS films. The increase in the Int EDP for the latter can be apparent or real or combination of both. The apparent increase can be realized due to the decrease in the film area, which comes into the calculation. This can happen when the voids of size (L_V) comparable to the coherent length scale (ξ) of the X-rays is present

in the film. Then the coherent scattering is replaced by the incoherent scattering (Ref. 2). The intensity of coherent scattering (I_{C}) is represented by amplitude addition, while that of incoherent scattering (I_{IC}) is represented by intensity addition, as follows

$$I_{\mathrm{C}} = |A_1 + A_2|^2, \tag{S4}$$

$$I_{\mathrm{IC}} = I_1 + I_2 = |A_1|^2 + |A_2|^2 \approx I_1, \tag{S5}$$

where A_1 and A_2 are the scattering amplitudes from the islands and voids of the film, respectively, while I_1 and I_2 are corresponding scattering intensities. When $L_V < \xi$ then Eq. S4 is valid, where total area of the film take part in ρ calculation, but when $L_V \geq \xi$ then Eq. S5 is valid, where the area corresponding to the large voids contribute in I_2 but not in the I_1. In the XR data analysis, where constant area is considered, the effective covered area reduction (due to increase in void size) in I_1 is then showed up as materials increment. On the other hand, the real increase of the Int EDP can be realized due to some kind of materials growth and/or attachment with time. It is known that the H-terminated Si surface is unstable and an oxide layer can grow with time (Ref. 3). The thickness of which can range up to nm. Moreover, due to such change in the nature of the substrate surface (from hydrophobic to hydrophilic) moisture can be attracted and attached. In the DT-AuNP/H-Si LS films, the growth of such hygroscopic oxide layer on the substrates can take place in and near the voids region of the films, which can then enhance the Int EDP. The less heights of the monolayer with respect to the voids in the DT-AuNP/H-Si LS films (Fig. S2) compared to the DT-AuNP/OTS-Si LS films (Fig. 2) indeed suggest the growth of oxide layer on the voids region of the H-Si substrates. The increase in the Int EDP with time for the DT-AuNP/H-Si LS films is probably due to the combination of both. The oxide layer growth is applicable for all the voids, while the additional incoherent scattering concept is applicable only to the large size voids (i.e. $L_V \geq \xi$, where ξ is in the μm range), which are only present in the films deposited at low Π values (see AFM images in Ref. 1).

References

[1]M. Mukhopadhyay and S. Hazra, *RSC Adv.*, 2016, **6**, 12326–12336

[2]S. Hazra, A. Gibaud, A. Désert, V. Gacem and N. Cowlam, *Physica B*, 2000, **283**, 45–48

[3]J. K. Bal and S. Hazra, *Phys. Rev. B*, 2007, **75**, 205411.